

Synthesis and Structure of the Hafnium Alkylidene Complex $[P_2Cp]Hf=CHPh(Cl)$ ($[P_2Cp] = (\eta^5-C_5H_3-1,3-(SiMe_2CH_2PPr^i_2)_2)$)

Michael D. Fryzuk,* Paul B. Duval, Brian O. Patrick,[†] and Steven J. Rettig[†]

Department of Chemistry, University of British Columbia, 2036 Main Mall, Vancouver, British Columbia, Canada V6T 1Z1

Received September 1, 2000

The synthesis, structural characterization, and solution behavior of hafnium complexes stabilized by the potentially tridentate ancillary ligand $[P_2Cp]$ ($[P_2Cp] = (\eta^5-C_5H_3-1,3-(SiMe_2-CH_2PPr^i_2)_2)$) are described. The reaction of $[P_2Cp]Li$ with $HfCl_4(THT)_2$ produces the hafnium trichloride complex $[P_2Cp]HfCl_3$ (**1**), the structure of which was determined by X-ray crystallography. Trichloride **1** is isostructural with the analogous zirconium complex $[P_2Cp]ZrCl_3$ (**2**) in the solid state, but in solution **1** exists as an equilibrium mixture of two isomers that interconvert by fluxional phosphine coordination. Treatment of **1** with 2 equiv of KCH_2Ph , followed by thermolysis, yields the first structurally characterized hafnium alkylidene complex, $[P_2Cp]Hf=CHPh(Cl)$ (**3**). A crystal structure determination obtained for **3** shows this complex to be isostructural with the zirconium analogue $[P_2Cp]Zr=CHR(Cl)$ (**4**). The primary difference between the Hf systems presented here and the previously studied Zr analogues is that metal–ligand bonding is stronger in the former, which accounts for shorter bond distances, a greater degree of chemical inertness, and the divergent solution behaviors observed for the trichloride derivatives **1** and **2**.

Introduction

Among the transition metals, zirconium and hafnium comprise two congeners whose chemical properties in some instances seem virtually indistinguishable. The similarities are largely attributed to the nearly identical ionic radii of Zr^{4+} and Hf^{4+} (1.45 Å), arising from Hf being the first element that succeeds the lanthanides and the associated lanthanide contraction.¹ Where chemical differences have been noted, these usually relate to stronger metal–ligand σ -bonding in the Hf complexes due to 6s orbital contraction emanating from relativistic effects. In general, the resulting trend is for Hf to be relatively inert in comparison to Zr and for comparatively shorter bond distances in the Hf complexes. Given the similar size of the two metals, this latter effect can induce steric crowding in the Hf coordination sphere when bulky ligands are employed, leading to structural modifications with respect to the analogous Zr complex. One example is illustrated by the homoleptic tetra(cyclopentadienyl) derivatives Cp_4M ($M = Zr,$ ² Hf ³), where only two of the Cp ligands coordinate with η^5 hapticity to Hf, in comparison to three η^5 -Cp ligands observed for the Zr species.

Our current interest in hafnium coordination chemistry derives from previous work from our laboratory

conducted on zirconium complexes stabilized by the ancillary ligand $[P_2Cp]$ ($[P_2Cp] = (\eta^5-C_5H_3-1,3-(SiMe_2-CH_2PPr^i_2)_2)$). Starting from the precursor trichloride complex $[P_2Cp]ZrCl_3$ (**2**), a variety of alkyl complexes of the general formula $[P_2Cp]ZrCl_{3-x}R_x$ ($x = 1, 2, 3$; $R = Me, CH_2Ph, CH_2SiMe_3$) have been prepared.^{4,5} The dialkyl derivatives $[P_2Cp]ZrClR_2$ are unique in that, in certain cases, they yield rare Zr alkylidene complexes in high yield upon thermolysis.^{5,6} Given that stable hafnium alkylidene complexes are currently unknown, we considered whether the generality of the zirconium alkylidene syntheses with this ancillary ligand system could be extended to include new Hf derivatives. Herein we report the synthesis and structural characterization of the Hf complex $[P_2Cp]HfCl_3$ (**1**), which serves to generate alkyl derivatives and the first example of a stable Hf alkylidene complex, $[P_2Cp]Hf=CHPh(Cl)$ (**3**). Although much of the reactivity and structural features of the Hf complexes mimic those of the Zr systems, an intriguing difference in solution behavior between the isostructural trichloride derivatives **1** and **2** is observed. A combination of steric factors associated with the bulky ancillary ligand and stronger metal–ligand binding in **1**, together with the option of fluxional sidearm phosphine coordination, are likely responsible for these observed differences.

[†] Professional Officers: UBC X-ray Structural Laboratory; S.J.R. deceased October 27, 1998.

(1) Cotton, F. A.; Wilkinson, G.; Murillo, C. A.; Bochmann, M. *Advanced Inorganic Chemistry*, 6th ed.; Wiley: New York, 1999; p 878.

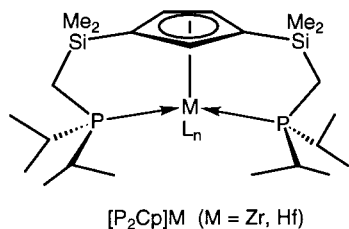
(2) Rogers, R. D.; Bynum, R. V.; Atwood, J. L. *J. Am. Chem. Soc.* **1978**, *100*, 5238.

(3) Rogers, R. D.; Bynum, R. V.; Atwood, J. L. *J. Am. Chem. Soc.* **1981**, *103*, 692.

(4) Fryzuk, M. D.; Mao, S. S. H.; Duval, P. B.; Rettig, S. J. *Polyhedron* **1995**, *14*, 11.

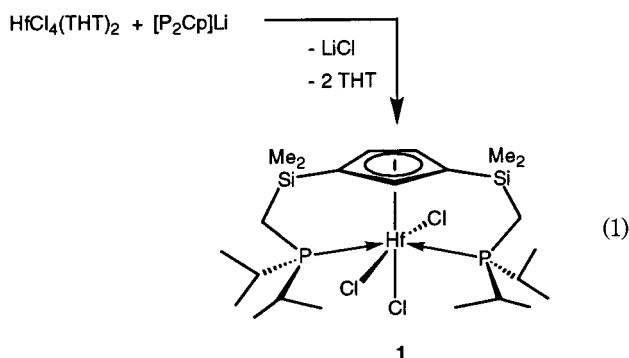
(5) Fryzuk, M. D.; Duval, P. B.; Mao, S. S. H.; Zaworotko, M. J.; MacGillivray, L. R. *J. Am. Chem. Soc.* **1999**, *121*, 2478.

(6) Fryzuk, M. D.; Mao, S. S. H.; Zaworotko, M. J.; MacGillivray, L. R. *J. Am. Chem. Soc.* **1993**, *115*, 5336.



Results and Discussion

Synthesis and Structure of [P₂Cp]HfCl₃ (1). The stoichiometric reaction of the ligand [P₂Cp]Li with HfCl₄(THT)₂ (THT = tetrahydrothiophene) in toluene at 65 °C for 24 h produces the Hf trichloride complex [P₂Cp]HfCl₃ (1) in high yield as colorless air- and moisture-sensitive crystals (eq 1). In contrast to this sluggish reaction, formation of the Zr analogue [P₂Cp]-ZrCl₃ (2) is complete within 12 h at room temperature.⁴



An X-ray crystal structure determination was obtained for the Hf trichloride derivative **1**. The molecular structure is shown in Figure 1, and a summary of the crystallographic data is given in Table 1. The Hf complex **1** is isostructural in the solid state with the previously characterized Zr derivative **2**; therefore, selected bond lengths and bond angles are presented for both **1** and **2** in Table 2 for comparison. The angular parameters for **1** and **2** are indeed very similar. However, the corresponding metal–ligand bond distances are approximately 0.02 Å shorter for the hafnium derivative, a feature that reflects a general trend of stronger ligand bonding to Hf versus Zr. The monomeric, quasi-octahedral geometry (given the cyclopentadienyl donor as occupying one coordination site) has been similarly observed in other structurally characterized adducts of the general formula CpMCl₃(L)₂ (M = Zr, Hf),^{7,8} including examples in which one⁹ or both¹⁰ of the donor atoms are appended to the cyclopentadienyl ring via a sidearm tether. The equatorial M–Cl and M–P bonds in **1** are directed away from the Cp ring toward the axial chloride, so that the P(1)–M(1)–P(1) and Cl(1)–M(1)–Cl(2) angles are distorted from idealized octahedral geometry by approximately 20°, a structural mode that is prevalent for mono(cyclopentadienyl) complexes.¹¹

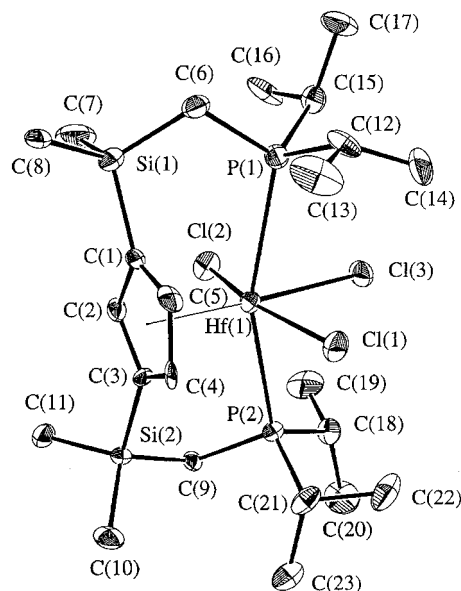


Figure 1. ORTEP view of **1**, showing 33% probability thermal ellipsoids for the non-hydrogen atoms.

Table 1. Crystallographic Data^a

	1	3
formula	C ₂₃ H ₄₇ Cl ₃ HfP ₂ Si ₂	C _{33.50} H ₅₇ ClHfP ₂ Si ₂
fw	726.59	791.88
cryst syst	orthorhombic	triclinic
space group	P2 ₁ 2 ₁ 2 ₁ (No. 19)	P1̄ (No. 2)
a, Å	13.760(4)	11.7554(11)
b, Å	15.8367(12)	12.488(2)
c, Å	14.274(2)	13.9584(10)
α, deg	90	98.3839(7)
β, deg	90	95.0101(9)
γ, deg	90	111.100(3)
V, Å ³	3110.6(10)	1869.5(3)
Z	4	2
D _{calc} , g/cm ³	1.551	1.407
F(000)	1464	810
μ, cm ⁻¹	3.772	30.26
cryst size, Å	4.0 × 3.5 × 1.5	4.5 × 3.5 × 1.5
transmn factors	0.686–1.000	0.92–1.00
scan type	ω–2θ	ω–2θ
scan range, deg in ω	0.95+0.35 tan θ	1.00+0.35 tan θ
data collected	±h, ±k, +l	±h, ±k, ±l
2θ _{max} , deg	32.5	60.1
total reflections	6212	15 781
independent reflns	6212	8376
no. with I ≥ 3σ(I)	2494	6427
no. of variables	280	374
R ₁ (F ²) (all data)	0.0415	0.069
R _w (F ²) (all data)	0.0343	0.072
gof	1.40	1.82
residual density, e/Å ³	–1.45 to 0.92	–2.97 to 2.47

^a Temperature 294 K, Rigaku AFC6S diffractometer, Mo Kα radiation (λ = 0.71069 Å), graphite monochromator, takeoff angle 6.0°, aperture 6.0 × 6.0 mm at a distance of 285 mm from the crystal, stationary background counts at each end of the scan (scan/background time ratio 2:1), σ²(F²) = [S²(C + 4B)]/Lp² (S = scan rate, C = scan count, B = normalized background count), function minimized Σw(|F_o – |F_c||)² where w = 4F_o²/σ²(F_o²), R(F) = Σ|F_o – |F_c||/Σ|F_o|, R_w(F) = (Σw(|F_o – |F_c||)²/Σw|F_o|²)^{1/2}, and gof(F) = [Σw(|F_o – |F_c||)²/(m – n)]^{1/2}.

Solution Behavior of [P₂Cp]HfCl₃ (1). Although the trichloride complexes **1** and **2** are isostructural in the solid state, the solution behavior of these species as measured by multinuclear NMR spectroscopy differs

(7) Lund, E. C.; Livinghouse, T. *Organometallics* **1990**, *9*, 2426.
 (8) Erker, G.; Sarter, C.; Albrecht, M.; Dehnicke, S.; Krüger, C.; Raabe, E.; Schlund, R.; Benn, R.; Rufinska, A.; Mynott, R. *J. Organomet. Chem.* **1990**, *382*, 89.
 (9) Zeijden, A. A. H.; Mattheis, C.; Fröhlich, R.; Zippel, F. *Inorg. Chem.* **1997**, *36*, 4444.
 (10) Mu, Y.; Piers, W. E.; MacGillivray, L. R.; Zaworotko, M. J. *Polyhedron* **1995**, *14*, 1.

(11) Winter, C. H.; Zhou, X.-X.; Dobbs, D. A.; Heeg, M. J. *Organometallics* **1991**, *10*, 210.

Table 2. Selected Bond Lengths (Å) and Bond Angles (deg) for $[P_2Cp]MCl_3$ (1: $M = Hf$, 2: $M = Zr$)^a

	1	2		1	2
M–Cl(1)	2.466(3)	2.489(1)	Cl(1)–M–Cl(2)	160.6(1)	160.61(5)
M–Cl(2)	2.476(3)	2.490(1)	Cl(1)–M–Cl(3)	80.7(1)	80.79(3)
M–Cl(3)	2.514(3)	2.529(1)	Cl(2)–M–Cl(3)	81.1(1)	81.19(5)
M–P(1)	2.876(4)	2.897(1)	P(1)–M–P(2)	159.3(1)	159.53(4)
M–P(2)	2.847(4)	2.871(1)	Cl(3)–M–P(1)	78.1(1)	78.32(4)
M–Cp'	2.25	2.260(5)	Cl(3)–M–P(2)	81.4(1)	81.43(4)
			Cp'–M–Cl(3)	177.4	177.50

^a Numbering scheme is identical for each.

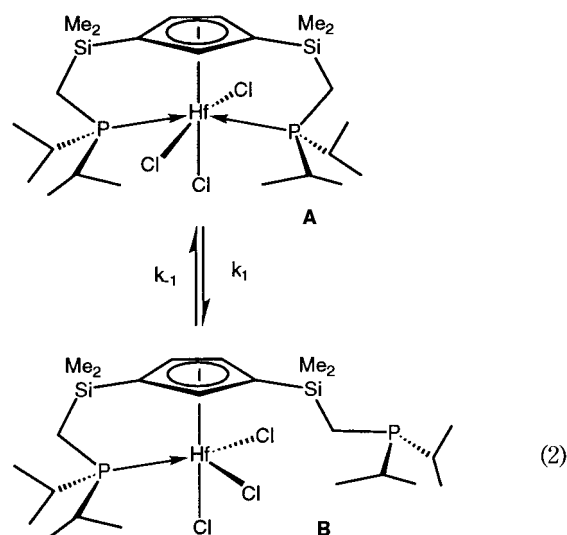
markedly. The $^{31}P\{^1H\}$, $^{13}C\{^1H\}$, and 1H NMR spectra of the Zr derivative **2** are consistent with the solid state structure and remain unchanged over the temperature range studied (-90 to 95 °C).⁴ For example, the $^{31}P\{^1H\}$ NMR spectrum of **2** shows a singlet at 10.7 ppm for two equivalent phosphines coordinated to the metal center. In the 1H NMR spectrum there are two cyclopentadienyl proton resonances in a 2:1 ratio due to the C_s symmetry of the complex, along with two peaks for the silylmethyl ($Si(CH_3)_2$) protons, two for the methylene (PCH_2Si) protons, and four peaks for the isopropyl ($PCH(CH_3)_2$) protons of the ligand backbone.

In contrast to the straightforward solution behavior observed for **2**, the temperature-dependent NMR spectroscopic features of the Hf derivative **1** are more complex. For example, the room-temperature $^{31}P\{^1H\}$ -NMR spectrum of **1** shows three broad resonances at -4.9 , 14.9 , and 24.9 ppm, in an approximate 1:2:1 ratio, respectively, in comparison to the sharp singlet seen for **2**. The peaks in the room-temperature 1H NMR spectrum for **1** are extremely broad and do not permit structural assignments. One possibility to account for these observations is that more than one isomer is present in solution at this temperature, with the broad resonances ascribed to exchange processes that interconvert these species.¹²

$^{31}P\{^1H\}$ and 1H NMR spectra were obtained for **1** at various temperatures to probe any temperature-dependent solution behavior associated with chemical exchange. As the temperature is lowered below room temperature, the peaks in the ^{31}P NMR spectrum gradually sharpen, and the two resonances at -4.9 and 24.9 ppm decrease in intensity relative to the other peak at 14.9 ppm. This trend continues until only the sharp singlet at 14.9 ppm is detected below -65 °C. This singlet can be assigned to a molecular structure as depicted in Figure 1, as the 1H NMR spectrum for **1** at this temperature shows well-defined peaks in an overall pattern that resembles closely the room-temperature 1H NMR spectrum of the Zr derivative **2**. For the following discussion this isomer will be designated as **A**.

The other two peaks at -4.9 and 24.9 ppm in the room-temperature $^{31}P\{^1H\}$ NMR spectrum for **1** evidently belong to another single isomer, as they are related by equivalent line shapes and integration in the NMR spectra obtained at various temperatures. The downfield peak at 24.9 ppm suggests a strongly coordinating phosphine donor, while the other peak at -4.9 ppm is indicative of an unbound phosphine for this ligand system. A five-coordinate structure as shown

below in **B** (eq 2) is consistent with the data. Variable-temperature 1H NMR spectroscopy also supports this proposed structure, as above -65 °C the emergence of new resonances consistent with the lower symmetry presented by **B** can be discerned. For example, separate singlets are observed for four inequivalent silylmethyl groups, and the three cyclopentadienyl protons are inequivalent. Assignment of the remaining resonances for **B** in the 1H NMR spectrum at these lower temperatures is complicated by the coexistence of **A**, and analysis is hampered further as the temperature is raised due to the associated increase in line broadening.



It is apparent from the NMR spectral data that the two isomers **A** and **B** are in equilibrium (eq 2). The former is exclusively favored at low temperatures, while the relative concentration of the latter increases as the temperature is raised. The broadened resonances in the $^{31}P\{^1H\}$ and 1H NMR spectra for this system arise because the fluxional process that interconverts these species occurs at a rate that is comparable to the NMR time scale. A similar equilibrium process has been noted for the zirconium trimethyl complex $[P_2Cp]ZrMe_3$.⁴ To evaluate the equilibrium in eq 2, the concentration of each species was measured at separate temperatures in the range between -65 and 20 °C, for which reliable measurements could be made from integration of the $^{31}P\{^1H\}$ NMR spectra. Equilibrium constants were calculated according to the equation $K = [B]/[A]$ and plotted as a function of temperature. The resulting van't Hoff plot is shown in Figure 2, from which the thermodynamic parameters $\Delta H^\circ = 4.9(5)$ kcal mol⁻¹ and $\Delta S^\circ = 17(1)$ cal mol⁻¹ K⁻¹ were obtained. The errors were estimated from separate experimental runs and indicate reproducibility. The positive entropy term is in accord with a less-ordered structure for **B**, represented by the dangling pendant sidearm and the overall lower symmetry of this molecule.

The different solution behavior exhibited by the isostructural derivatives **1** and **2** offers a unique example of the subtle electronic differences between Zr and Hf, the two elements that are considered to be the most similar in chemical behavior among the transition metals. A comparison of the solid state structures of these trichloride complexes shows that the corresponding bond distances are shorter in Hf **1**, presumably due

(12) Sandstrom, J. *Dynamic NMR Spectroscopy*; Academic Press: New York, 1982.

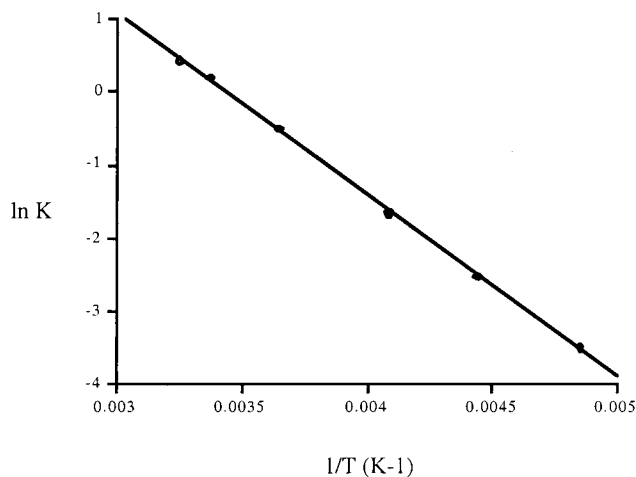
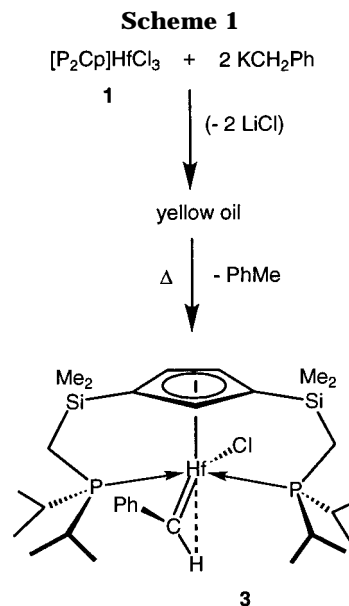


Figure 2. van't Hoff plot for the equilibrium shown in eq 2, based on the $^{31}\text{P}\{^1\text{H}\}$ NMR spectral data.

to stronger ligand binding. The more open coordination sphere in **B** may therefore relieve steric pressures arising from the close Hf-ligand contacts in the quasi-octahedral geometry present in **A**, a process that is absent in the less sterically encumbered Zr derivative **2**. The observed equilibrium mixture of **A** and **B** in solution for **1** reflects the fact that the two geometries are energetically comparable ($\Delta G^\circ = -0.1(5)$ kcal mol $^{-1}$). As mentioned earlier, other examples have been noted where structural differences exist between Zr and Hf analogues of the same general formula. For the tetra-(cyclopentadienyl) complexes Cp_4M ($\text{M} = \text{Zr},^2 \text{Hf}^3$), as with **1** and **2**, adopting a less crowded geometry may be a similar steric response to stronger metal-ligand bonding in the Hf derivative.

Synthesis and Molecular Structure of $[\text{P}_2\text{Cp}]\text{Hf}=\text{CHPh}(\text{Cl})$ (3**).** We have previously reported the synthesis and molecular structure of the first structurally characterized zirconium alkylidene complexes $[\text{P}_2\text{Cp}]\text{Zr}=\text{CHR}(\text{Cl})$ ($\text{R} = \text{Ph}, \text{SiMe}_3$). 5,6 As described below, these systems have now been extended to include the first structurally characterized hafnium alkylidene complex $[\text{P}_2\text{Cp}]\text{Hf}=\text{CHPh}(\text{Cl})$ (**3**). The reaction of trichloride **1** with 2 equiv of KCH_2Ph generates a complex mixture of hafnium alkyl species, the nature of which will be discussed later. Thermolysis of this reaction mixture in toluene for 6 days at 95 °C produces the alkylidene complex **3** in high yield (Scheme 1), which can be isolated as air-sensitive crystals from cold hexanes. As observed in comparing the formation of the trichloride species **1** and **2**, generation of the Hf benzylidene derivative is considerably slower in comparison to the analogous Zr complex $[\text{P}_2\text{Cp}]\text{Zr}=\text{CHPh}(\text{Cl})$ (**4**), 6 where the reaction is complete within 12 h at 65 °C.

Single crystals of Hf benzylidene **3** suitable for X-ray diffraction were obtained by slow cooling of a hexanes solution. The data collection and crystallographic parameters are summarized in Table 1, and selected bond lengths and bond angles are given in Table 3 along with those of the Zr benzylidene complex **4** for comparison. The molecular structure of **3** is depicted in Figure 3. As with the trichlorides **1** and **2**, the Hf benzylidene **3** is isostructural with the Zr derivative **4**, and again the corresponding bond lengths are shorter for the Hf complex. The alkylidene unit in **3** is directed *syn* to the unique cyclopentadienyl carbon; this stereochemical



preference has been noted before with the $[\text{P}_2\text{Cp}]$ ligand set. 13 A very short Hf(1)–C(24) bond distance of 1.994–(4) Å is indicative of metal–ligand multiple bonding in the alkylidene moiety. For comparison, a typical Hf–C single bond averages approximately 2.30 Å. 1 A characteristic feature of metal alkylidene complexes is an α -agostic C–H interaction to the metal center. 14 For both derivatives the position of the α -hydrogen atom was located and refined (for **3**, this atom was refined with restraints). The short Hf(1)⋯H(48) contact of 1.93–(3) Å for **3** is characteristic for an α -agostic bond, which is also reflected in an open Hf(1)–C(24)–C(25) bond angle of nearly 170°. The agostic interaction orients the benzylidene unit such that the phenyl ring points toward the cyclopentadienyl portion of the ancillary ligand. The phenyl ring is aligned perpendicular to the Cp ring, both to minimize steric interactions with the bulky isopropyl groups on the sidearm phosphines and to maximize orbital overlap with the metal. In comparison to the trichloride derivative **1**, the absence of an axial ligand *trans* to the cyclopentadienyl donor in **3** (compensated somewhat by the agostic C–H interaction at this site) results in a modified geometry approaching that of a typical four-legged piano stool. Therefore the angular distortion of the equatorial bonds away from the Cp ring is increased in **3** relative to trichloride **1** and is particularly evident with the *trans* chloride and alkylidene ligands, where the Cl(1)–Hf(1)–C(24) bond angle is less than 110°.

The NMR spectroscopic data for benzylidene **3** are consistent with the solid state structure. A singlet is seen in the $^{31}\text{P}\{^1\text{H}\}$ NMR spectrum at 23.4 ppm for a pair of equivalent metal-bound phosphines, and the ^1H NMR spectrum exhibits peaks for the ancillary ligand as expected for a molecule with C_s symmetry. Diagnostic of the alkylidene unit are the downfield resonances for both the α -carbon atom (210 ppm) and α -hydrogen atom (7.33 ppm) in the respective ^{13}C and ^1H NMR spectra.

(13) Fryzuk, M. D.; Duval, P. B.; Mao, S. S. H.; Rettig, S. J.; Zaworotko, M. J.; MacGillivray, L. R. *J. Am. Chem. Soc.* **1999**, *121*, 1707.

(14) Wilkinson, G.; Stone, F. G. A.; Abel, E. W. *Comprehensive Organometallic Chemistry*, 2nd ed.; Pergamon Press: Oxford, 1995; Vol. 5, Chapter 2.

Table 3. Selected Bond Lengths (Å) and Bond Angles (deg) for $[P_2Cp]M=CHPh(Cl)$ (**3**: M = Hf, **4**: M = Zr)^a

	3	4		3	4
M(1)–Cl(1)	2.5068(11)	2.5418(13)	Cl(1)–M(1)–P(1)	75.90(4)	77.23(4)
M(1)–P(1)	2.8038(14)	2.8299(16)	Cl(1)–M(1)–P(2)	76.79(4)	76.35(4)
M(1)–P(2)	2.7986(13)	2.8425(17)	P(1)–M(1)–P(2)	152.68(4)	153.58(4)
M(1)–C(24)	1.994(4)	2.024(4)	Cl(1)–M(1)–C(24)	108.87(13)	110.11(11)
C(24)–C(25)	1.481(5)	1.456(5)	M(1)–C(24)–C(25)	167.8(4)	169.2(3)
M(1)–Cp'	2.22	2.234	M(1)–C(24)–H(48)	71.6(17)	79.8(23)
M(1)⋯H(48)	1.93(3)	2.07(4)			

^a Numbering scheme is identical for each.

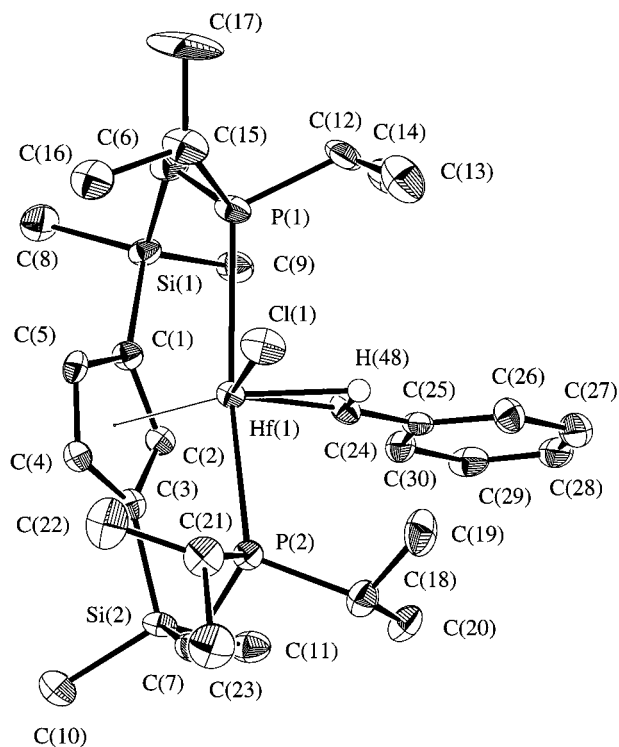


Figure 3. ORTEP view of **3**, showing 33% probability thermal ellipsoids for the non-hydrogen atoms and H(48).

A previous examination of the formation of the Zr alkylidene complexes $[P_2Cp]Zr=CHR(Cl)$ ($R = Ph, SiMe_3$) revealed a composite mechanism.⁵ The dialkyl complex was determined to be the direct precursor that underwent α -abstraction to give the alkylidene product, but a complicating preequilibrium involving all three alkyl species was observed in synthetic attempts to isolate the dialkyl precursor. Similarly, the reaction of trichloride **1** with KCH_2Ph yields a mixture of alkyl species. The identity of two of these complexes as mono(benzyl) $[P_2Cp]HfCl_2(CH_2Ph)$ (**5**) and tris(benzyl) $[P_2Cp]Hf(CH_2Ph)_3$ (**7**) has been confirmed by independent syntheses using the appropriate stoichiometry of the alkylating reagent. Mono(benzyl) **5** is produced as a slightly impure oil, while tris(benzyl) **7** is obtained in good yield as an air-sensitive oil. Both of these species resemble the previously characterized Zr analogues, based on a comparison of the NMR spectroscopic data. Unfortunately, in contrast to the Zr systems, where the dialkyl derivatives could be assigned from the NMR spectra, the analogous hafnium bis(benzyl) complex $[P_2Cp]HfCl_2(CH_2Ph)_2$ (**6**) could not be positively identified from the reaction mixture. However, given the overall similarities noted in the Zr and Hf systems, it seems likely that alkylidene formation of **3** follows a course similar to that depicted for the zirconium analogue.

Concluding Remarks

Utilization of the multidentate ancillary ligand $[P_2Cp]$ has been extended to include an examination of its coordination chemistry with hafnium, with the synthesis of trichloride, benzyl, and benzylidene complexes. Although Hf alkylidene complexes have been inferred as reactive intermediates,¹⁵ benzylidene **3** is the first example of a structurally characterized Hf alkylidene complex. The reactions that produce the Hf derivatives are found to be considerably more sluggish than the corresponding reactions that generate the Zr analogues, in accord with the more inert chemical properties of Hf. X-ray crystallographic determinations revealed that the hafnium trichloride complex **1** and the benzylidene complex **3** are isostructural to their zirconium analogues **2** and **4**, respectively, in the solid state. However, shorter metal–ligand bond distances were found for the Hf species, reflecting a trend that is generally observed between these two congeners, that ligands form stronger bonds to Hf relative to Zr. Despite the similar solid state structures, the complex fluxional solution behavior exhibited by the Hf trichloride derivative **1** differs significantly from the Zr analogue **2**. The equilibrium mixture of isomers seen for **1** is likely a response to alleviate steric congestion arising from the above-noted closer metal–ligand contacts.

Experimental Section

General Considerations. All manipulations were performed under an atmosphere of prepurified nitrogen in a Vacuum Atmospheres HE-553-2 glovebox equipped with a MO-40-2H purification system or in standard Schlenk-type glassware on a dual vacuum/nitrogen line. ¹H NMR spectra (referenced to nondeuterated impurity in the solvent) were performed on one of the following instruments depending on the complexity of the particular spectrum: Bruker WH-200, Varian XL-300, or Bruker AM-500. ¹³C NMR spectra (referenced to solvent peaks) were run at 75.429 MHz on the XL-300 instrument, and ³¹P NMR spectra (referenced to external $P(OMe)_3$ at 141.0 ppm) were run at 121.421 and 202.33 MHz, on the XL-300 and Bruker AM-500 instruments, respectively. All chemical shifts are reported in ppm, and all coupling constants are reported in Hz. Elemental analyses were performed by Mr. P. Borda of this department.

Reagents. Hexanes and tetrahydrofuran (THF) were pre-dried over CaH_2 followed by distillation from sodium benzophenone ketyl under argon. Toluene was dried over sodium under argon, and hexamethyldisiloxane was distilled from sodium benzophenone ketyl under nitrogen. The deuterated solvents C_6D_6 and $C_6D_5CD_3$ were dried over molten sodium, vacuum transferred, and degassed by freeze–pump–thaw

(15) Bulls, A. R.; Schaefer, W. P.; Serfas, M.; Bercaw, J. E. *Organometallics* **1987**, *6*, 1219.

technique before use. $\text{KCH}_2\text{Ph}^{16}$ and $[\text{P}_2\text{Cp}]\text{Li}^6$ were prepared according to literature methods.

$[\text{P}_2\text{Cp}]\text{HfCl}_3$ (1). Toluene (100 mL) was added to an intimate mixture of $[\text{P}_2\text{Cp}]\text{Li}$ (1.82 g, 4.06 mmol) and $\text{HfCl}_4\text{-(THT)}_2$ (2.02 g, 4.08 mmol) at 0 °C. The mixture was heated to 65 °C and stirred at that temperature for 24 h, during which the yellowish color of the ligand gradually diminished to give a pale buff yellow slurry. The mixture was filtered and the solvent reduced to 10 mL, from which pale yellow crystals were obtained at -78 °C. The crystals were washed with cold hexanes and dried. Yield: (1.99 g, 67%). Anal. Calcd for $\text{C}_{23}\text{H}_{47}\text{Cl}_3\text{HfP}_2\text{Si}_2$: C, 38.02; H, 6.52. Found: C, 38.40; H, 6.70. In solution, **1** exists as an equilibrium mixture consisting of two isomers (**A** and **B**).

Isomer A. ^1H NMR (-40 °C, C_7D_8): δ 0.12 and 0.38 (s, 6H, $\text{Si}(\text{CH}_3)_2$), 0.84 (dd, 4H, $^2J_{\text{HH}} = 6$ Hz, $^2J_{\text{PH}} = 4$ Hz, SiCH_2P), 0.99 and 1.34 (m, 12H, $\text{CH}(\text{CH}_3)_2$), 2.15 and 2.77 (sept., 2H, $^3J_{\text{HH}} = 7$ Hz, $\text{CH}(\text{CH}_3)_2$), 6.51 (d, 2H, $^4J_{\text{HH}} = 1$ Hz, Cp-H), 7.18 (t, 1H, $^4J_{\text{HH}} = 1$ Hz, Cp-H). ^{31}P NMR (-40 °C, C_7D_8): δ 14.9 (s).

Isomer B. ^1H NMR (-40 °C, C_7D_8): δ 0.08, 0.30, 0.68, and 0.71 (s, 3H, $\text{Si}(\text{CH}_3)_2$), 1.08 and 1.17 (m, 12H, $\text{CH}(\text{CH}_3)_2$), 1.52 and 1.84 (m, 2H, $\text{CH}(\text{CH}_3)_2$), 6.62, 6.66, and 7.12 (m, 1H, Cp-H). ^{31}P NMR (-40 °C, C_7D_8): δ -4.9 and 24.9 (br s).

$[\text{P}_2\text{Cp}]\text{Hf}=\text{CHPh}(\text{Cl})$ (3). A solution of KCH_2Ph (143 mg, 1.10 mmol) in 30 mL of THF was added dropwise with stirring to a cooled (-78 °C) solution of **1** (400 mg, 0.55 mmol) dissolved in 60 mL of THF. The color of the solution slowly changed to bright yellow. The solution was warmed to room temperature and then stirred for another 3 h. The solvent was then removed in vacuo, and the residue extracted with hexanes and filtered. The filtrate was reduced under vacuum to give a yellow oil, which was redissolved in 30 mL of toluene. This solution was placed in an oil bath at 95 °C for 6 days, after which time no further reaction could be detected by NMR spectroscopy (for a corresponding NMR scale reaction). The solvent was removed, and the oil extracted with hexanes to give a bright yellow solid, which yielded crystals suitable for X-ray diffraction from a toluene/hexanes solution mixture at -40 °C. Yield: 305 mg, 70%. ^1H NMR (20 °C, C_6D_6): δ 0.12 and 0.31 (s, 6H, $\text{Si}(\text{CH}_3)_2$), 0.42 and 0.49 (dd, 4H, $^2J_{\text{HH}} = 5$ Hz, $^2J_{\text{PH}} = 7$ Hz, SiCH_2P), 0.79, 0.96, 1.33 and 1.14 (dd, 6H, $^3J_{\text{HH}} = 7$ Hz, $^3J_{\text{PH}} = 6$ Hz, $\text{CH}(\text{CH}_3)_2$), 1.73 and 2.43 (m, 2H, $\text{CH}(\text{CH}_3)_2$), 6.11 (t, 1H, $^4J_{\text{HH}} = 1$ Hz, Cp-H), 6.67 (t, 1H, $^3J_{\text{HH}} = 7$ Hz, p- C_6H_5), 7.09 (d, 2H, $^4J_{\text{HH}} = 1$ Hz, Cp-H), 7.16 (t, 2H, $^3J_{\text{HH}} = 7$ Hz, m- C_6H_5), 7.33 (s, 1H, CHPh), 7.45 (d, 2H, $^4J_{\text{HH}} = 7$ Hz, o- C_6H_5). ^{31}P NMR (20 °C, C_6D_6): δ 23.4 (s). Anal. Calcd for $\text{C}_{30}\text{H}_{53}\text{ClHfP}_2\text{Si}_2(\text{C}_7\text{H}_8)_{0.5}$: C, 50.81; H, 7.25 Found: C, 50.86; H, 7.51.

$[\text{P}_2\text{Cp}]\text{HfCl}_2(\text{CH}_2\text{Ph})$ (5). A solution of KCH_2Ph (115 mg, 0.88 mmol) in 30 mL of THF was added dropwise to a cooled (-78 °C) stirring solution of **1** (650 mg, 0.89 mmol) dissolved in 60 mL of THF. The colorless Hf solution gradually turned yellowish-orange. The mixture was allowed to warm to room temperature and then stirred for 12 h. The volatiles were then removed under vacuum, and the residue was extracted with hexanes and filtered. Removal of the solvent under vacuum yielded an impure yellowish oil, soluble in pentane, consisting of approximately 80% **5** by NMR spectroscopy. ^1H NMR (20 °C, C_6D_6): δ 0.02 (s, 12H, $\text{Si}(\text{CH}_3)_2$), 0.24 and 0.60 (d, 2H, $^2J_{\text{PH}} = 5$ Hz, SiCH_2P), 0.91 (m, 24H, $\text{CH}(\text{CH}_3)_2$), 1.55 (m, 4H, $\text{CH}(\text{CH}_3)_2$), 2.42 (s, 2H, CH_2Ph), 6.38 (d, 2H, $^4J_{\text{HH}} = 2$ Hz, Cp-H), 6.74 (t, 1H, $^4J_{\text{HH}} = 1$ Hz, Cp-H), 6.79 (t, 1H, $^3J_{\text{HH}} = 7$ Hz, p- C_6H_5), 7.23 (t, 2H, $^3J_{\text{HH}} = 7$ Hz, m- C_6H_5), 7.42 (d, 2H, $^3J_{\text{HH}} = 7$ Hz, o- C_6H_5). $^{31}\text{P}\{^1\text{H}\}$ NMR (-20 °C, C_7D_8): δ 0 and 19 (very br).

$[\text{P}_2\text{Cp}]\text{Hf}(\text{CH}_2\text{Ph})_3$ (7). A solution of KCH_2Ph (84 mg, 0.64 mmol) in 30 mL of THF was added dropwise over a period of 20 min to a cooled (-78 °C) stirring solution of **1** (156 mg, 0.21 mmol) dissolved in 30 mL of THF. The solution was allowed to slowly warm to room temperature and stirred for 12 h, during which the colorless Hf solution gradually turned bright yellow. The volatiles were then removed under vacuum, and the residue was extracted with hexanes and filtered. Removal of the solvent under vacuum yielded a hydrocarbon soluble yellowish oil. Yield: 135 mg, 72%. ^1H NMR (20 °C, C_6D_6): δ 0.34 (s, 12H, $\text{Si}(\text{CH}_3)_2$), 0.56 (d, 4H, $^2J_{\text{PH}} = 5$ Hz, SiCH_2P), 0.95 (m, 24H, $\text{CH}(\text{CH}_3)_2$), 1.50 (sept, 4H, $^2J_{\text{HH}} = 7$ Hz, $\text{CH}(\text{CH}_3)_2$), 1.90 (s, 6H, CH_2Ph), 6.28 (d, 2H, $^4J_{\text{HH}} = 2$ Hz, Cp-H), 6.69 (t, 1H, $^3J_{\text{HH}} = 2$ Hz, Cp-H), 6.78 (d, 6H, $^3J_{\text{HH}} = 7$ Hz, o- C_6H_5), 6.87 (t, 3H, $^3J_{\text{HH}} = 7$ Hz, p- C_6H_5), 7.17 (t, 6H, $^3J_{\text{HH}} = 7$ Hz, m- C_6H_5). $^{31}\text{P}\{^1\text{H}\}$ NMR (20 °C, C_6D_6): δ -5.6 (s). $^{13}\text{C}\{^1\text{H}\}$ NMR (20 °C, C_6D_6): δ -0.2 and 0.2 (s, $\text{Si}(\text{CH}_3)_2$), 8.1 (d, $^1J_{\text{PC}} = 35$ Hz, SiCH_2P), 16.5, 17.2, 17.4 and 18.0 (s, $\text{CH}(\text{CH}_3)_2$), 26.0 and 26.4 (d, $^1J_{\text{PC}} = 15$ Hz, $\text{CH}(\text{CH}_3)_2$), 70.1 (s, CH_2Ph), 121.6 (s, Cp), 130.1 (s, o- C_6H_5), 131.7 (s, m- C_6H_5), 140.9 (s, p- C_6H_5).

Acknowledgment. Financial support for this research was provided by NSERC of Canada in the form of a Research Grant to M.D.F. and a postgraduate scholarship to P.B.D.

Supporting Information Available: X-ray crystallographic files, in CIF format, for the structure determination of $[\text{P}_2\text{Cp}]\text{HfCl}_3$ (**1**) and $[\text{P}_2\text{Cp}]\text{Hf}=\text{CHPh}(\text{Cl})$ (**3**) are available. This material is available free of charge via the Internet at <http://pubs.acs.org>.

OM000760I

(16) Schlosser, M.; Hartmann, J. *Angew. Chem., Int. Ed. Engl.* **1973**, *12*, 508.